International Journal of Research in Agricultural Sciences
Volume 12, Issue 3, ISSN (Online): 2348 – 3997

Integrated use of Geospatial Technique and RUSLE Model for Soil Erosion Severity Areas Identification and Soil Loss Estimation for Selected Watershed of Bale Highland, Southeastern Ethiopia

Mulugeta Eshetu[1*], Tesfaye Ketema[2], Regassa Gosa[3] and Girma Getachew[4]
[1,2,3,4]Sinana Agricultural Research Center, Soil Fertility Improvement, Soil and Water Conservation and Watershed Management Team, P. O. Box 208, Bale-Robe, Ethiopia.
*Corresponding author email id: mulugeteshetu@gmail.com

Date of publication (dd/mm/yyyy): 16/06/2025

Abstract **– Soil erosion seriously threatened food security and agricultural sustainability, especially in Ethiopia's highlands, such as the Bale Highlands. The purpose of this study was to use the RUSLE model combined with GIS to estimate soil loss and identify zones of erosion severity in the watershed. Diverse methods and approaches were employed to generate model inputs, including slope length and steepness (LS), rainfall erosivity (R), soil erodibility (K), cover management (C), and conservation practices (P), which were derived from rainfall data, soil characteristi--cs, digital elevation models (DEM), and land use land cove maps. Although 82.84% of the land experiences slight soil loss, nearly 17% faces moderate to severe degradation, particularly in WS9 and WS10, which demand urgent intervention. A priority-based, site-specific soil and water conservation strategy is essential for sustainable land productivity. Effective soil and water conservation must be prioritized in erosion-prone sub-watersheds WS9 and WS10, with WS5 requiring targeted monitoring and WS6-WS8 needing moderate interventions. Sub-watersheds WS1-WS4 remain stable but demand continued protective management. RUSLE-integrated geospatial analysis proves vital for prioritizing site-specific, evidence-based conservation planning and should be complemented by long-term erosion monitoring.**

Keywords **– GIS, RUSLE, Soil Erosion, Sub-Watersheds.**

I. INTRODUCTION

Soils are essential for sustaining ecosystems and human livelihoods, offering critical environmental services (Allafta *et al*., 2022; Sud *et al*., 2024). Managing soil health is vital for sustainable agriculture and environmental resilience. However, soil erosion remains a global concern, leading to land degradation, reduced productivity, and water quality decline (Stefanidis *et al*., 2022; Thakuriah, 2023 and Eliyas *et al*., 2024). Water-induced soil erosion is a natural process where rainfall detaches and transports soil particles, leading to their deposition in downslope areas. Water-driven erosion, influenced by rainfall, topography, land use, and vegetation, displaces fertile soil from productive lands (Luvai *et al*., 2022 and Olika *et al*., 2023).

Developing countries face greater vulnerability to soil erosion due to their heavy reliance on agriculture, where soil degradation directly threatens food security, livelihoods, and environmental sustainability (Stefano *et al*., 2023; Li *et al*., 2024 and Sodoke *et al*., 2025). In Ethiopia's highland regions, soil erosion has led to substantial ecological degradation and socioeconomic losses over the past three decades (Eliyas *et al*., 2024). In the Bale highlands, improper agricultural practices have accelerated erosion, severely undermining soil fertility and crop productivity. The ongoing severity of this issue highlights the urgent need for well-planned soil and water conservation measures to safeguard both the environment and rural livelihoods.

Studies conducted in the Ethiopian highlands have demonstrated that soil erosion is a direct consequence of long-standing human settlement in the region (Hurni, 1993; Keesstra *et al*., 2016). The issue is further aggravated by inappropriate land use planning, unsustainable agricultural practices, and widespread deforestati--on. These factors collectively contribute to declining agricultural productivity, which in turn exacerbates food insecurity a persistent challenge in Ethiopia. Recent studies have shown that the mean annual soil loss in many parts of the Ethiopian highlands significantly exceeds the tolerable soil loss threshold, which ranges from 2 to 18 tons per hectare per year (t ha^{-1} y^{-1}), depending on land use, soil type, and topography (Hurni, 1985; FAO, 1986; Bewket and Sterk, 2005). This unsustainable rate of soil erosion leads to the depletion of topsoil, loss of soil fertility, and reduced water-holding capacity, which directly threaten agricultural productivity and rural livelihoods.

Currently, geospatial techniques such as remote sensing and GIS combined with the RUSLE model offer powerful tools for land and water resource planning, surpassing traditional methods in accuracy and efficiency (Arabameri *et al*., 2020). The integrating RUSLE with remote sensing and GIS technologies, the model's spatial resolution is significantly improved, allowing for more precise mapping of soil loss at a granular level. The Revised Universal Soil Loss Equation (RUSLE), developed by Renard *et al* (1997), is a robust and widely used empirical model for predicting long-term average annual soil loss. This integration is vital for identifying erosion hotspots and provides a scientific basis for prioritizing interventions and formulating effective soil and water conservation strategies.

Despite the limited information and documented studies on soil erosion severity and nutrient loss in the Bale highland watersheds, identifying regions most affected by soil erosion is critical for effective management. Using GIS and the RUSLE model to prioritize these areas and recommend suitable conservation strategies is essential. This study was initiated to estimate soil loss rates, identify areas with severe erosion, create a soil loss severity map, and prioritize regions for targeted soil conservation interventions using GIS and the RUSLE model.

II. Materials and Methods

The study was conducted in the Bale districts of Oromia Regional State, Ethiopia, specifically within the Sinana, Goba, Dinsho, and Agarfa sub-watersheds, located between 6°35-7°37′N and 39°40′-40°30′E (Figure 1). The area is characterized by highland agro-ecology with elevations ranging from 1,298 to 4,345 meters above sea level. It experiences a bimodal rainfall pattern (700-1400 mm/year), average temperatures of 9°C to 25°C, and supports mixed crop-livestock farming primarily barley, wheat, and livestock shaped by its undulating to mountainous topography.

Sub Watershed Classifications

The table (Table 1 and figure 2) presents the distribution of areas across different sub-watersheds, highlight--ing the size and relative percentage of each watershed within the study area. Watershed WS10 covers the largest area at 74,513.86 ha (27.25%), followed by WS9 at 63,640.17 ha (23.27%) and WS8 at 63,329.83 ha (23.16%), indicating these watersheds are the most significant in terms of spatial extent. Smaller watersheds such as WS1 (4,694.47 ha, 1.72%) and WS5 (6,053.06 ha, 2.21%) account for a relatively smaller portion of the total area, suggesting they may have different erosion dynamics and conservation needs compared to the larger watersheds. The variation in watershed sizes necessitates tailored management strategies to address soil erosion and conservation priorities specific to each sub-watershed's scale.

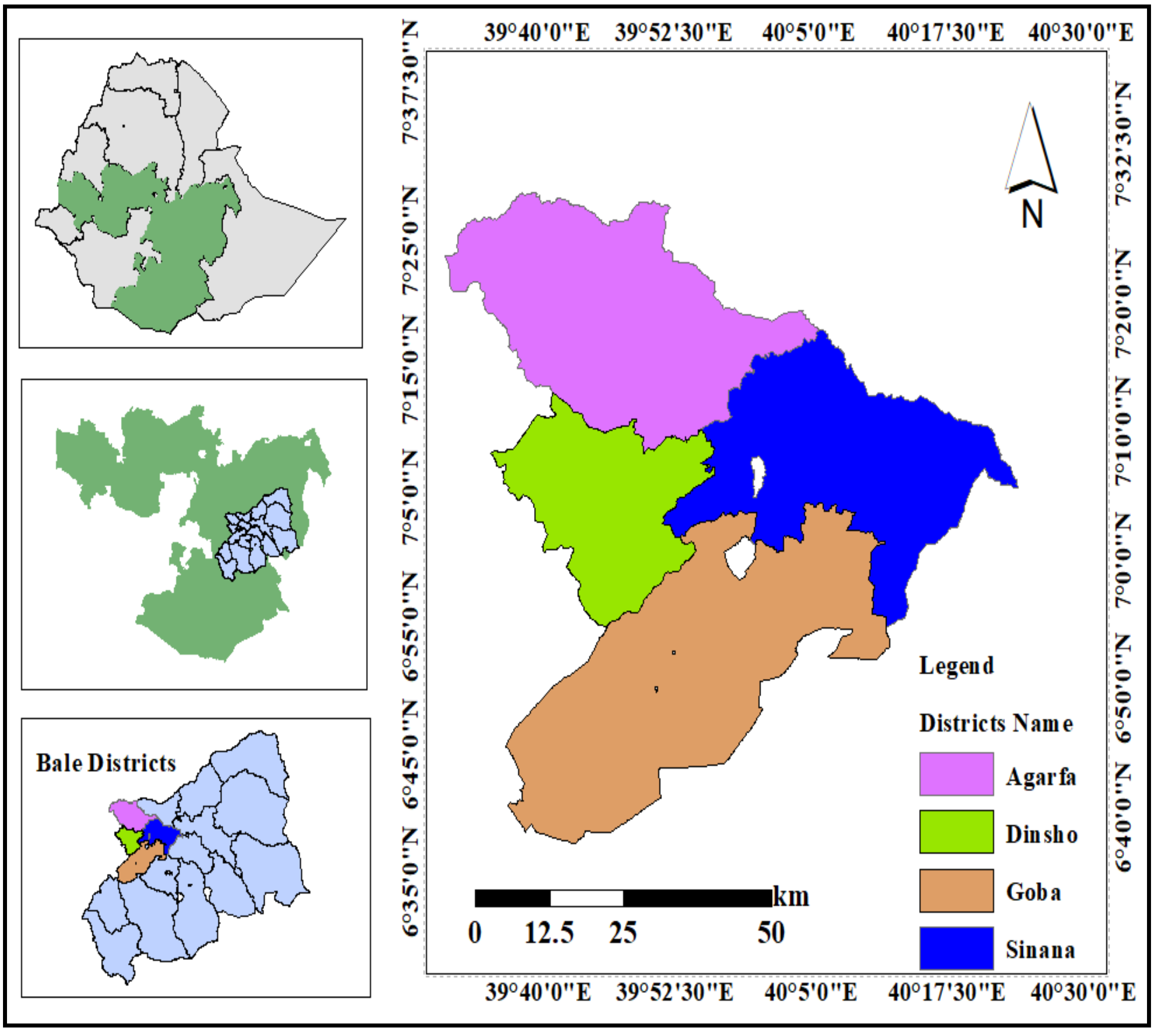

Fig. 1. Map of the study area.

Table 1. Descriptions of the selected Sub watershed classifications.

Sub Watersheds	Area (ha)	Area (%)
WS1	4694.47	1.72
WS2	6371.43	2.33
WS3	17709.42	6.48
WS4	19577.60	7.16
WS5	6053.06	2.21
WS6	10120.94	3.70
WS7	7482.03	2.74
WS8	63329.83	23.16
WS9	63640.17	23.27
WS10	74513.86	27.25

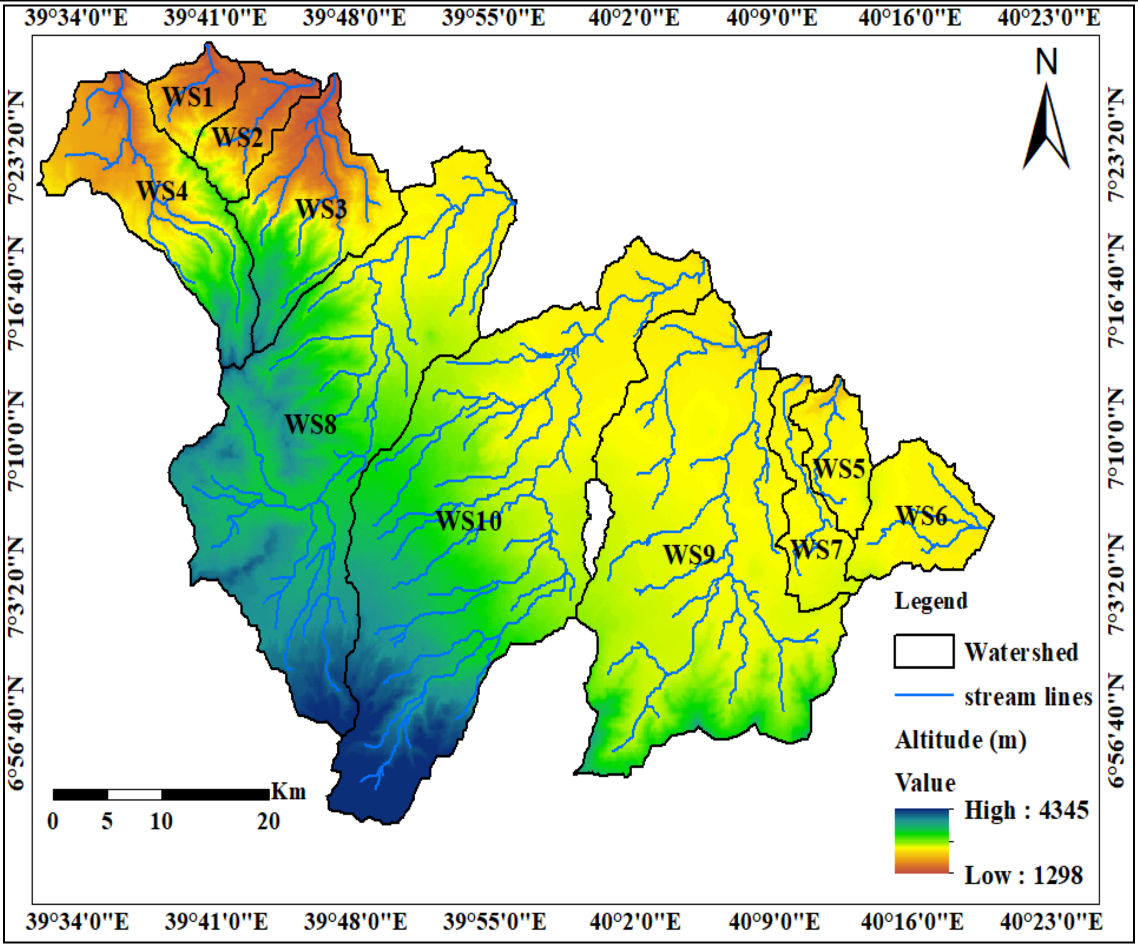

Fig. 2. Sub-watershed map and the drainage lines.

Data Type and Sources

The data types and sources used to estimate soil loss rates, identify areas with severe erosion, create a soil loss severity map, and prioritize regions for targeted soil conservation interventions using GIS and the RUSLE model are critical to ensuring the accuracy and reliability of the study's results. Rainfall data from meteorologi--cal stations calculates the R factor for erosion, while soil properties data assesses the K factor for soil erodibility. Topographic data from DEMs helps compute the LS factor, and land use data from satellite imagery evaluates vegetation's impact on erosion. Conservation practices data, gathered via surveys or remote sensing, informs management strategies. GIS integrates all these data types to map soil erosion severity and prioritize conservation actions.

Integrating these diverse data sources with GIS and the RUSLE model, the study can accurately estimate soil erosion rates, identify erosion-prone areas, and develop targeted conservation plans for specific areas in the Bale highland watersheds. This integrated approach ensures a comprehensive, data-driven strategy for soil and water conservation in the area.

Types of Software and Purpose

The RUSLE model relies on a range of software tools for effective data processing and analysis. GIS software such as ArcGIS and QGIS are used to integrate spatial data, allowing for the analysis of terrain and land use factors. Remote sensing tools like ERDAS IMAGINE are employed to analyze land cover and derive crucial terrain information, while Microsoft Excel is utilized for the necessary calculations involved in the RUSLE model (Table 2). These software tools work together to enhance the accuracy and efficiency of soil erosion assessments and the development of targeted conservation strategies.

Table 2. Types and purpose of software used.

Types of Software	Purpose
GPS	Ground truth data collections
Arc GIS 10.5	Spatial data analysis, mapping, and visualization. Integrates various data layers for RUSLE.
ERDAS Imagine 2015	Remote sensing software for processing satellite images and deriving land use/cover data.
RUSLE model	Compute annual soil erosion rates and its severity
Microsoft Excel	Data entry, calculations, and statistical analysis of RUSLE model parameters.

Inputs Analysis and Calculation

Rainfall Erosivity Factor

The Rainfall Erosivity Factor (R) was calculated using the empirical equation by Hurni (1985), as rainfall kinetic energy and I30 data were unavailable. The mean annual rainfall was interpolated using IDW in ArcGIS to create a continuous rainfall map, which has been widely applied in similar studies in Ethiopia (Tesfaye et al., 2018 and Belayneh et al., 2019). Finally, the R factor was computed using Equation (1) as presented below.

$$R = -8.12 + 0.562P \quad (1)$$

Where R is the rainfall erosivity factor (MJ mmha−1h−1) and P is the mean annual rainfall (mm).

Soil Erodibility Factor

The soil erodibility factor (K) indicates the soil's susceptibility to detachment and transport by runoff, mainly governed by its texture, organic carbon content, and permeability (Pham et al., 2018). Using soil laboratory results for organic carbon and texture, the K factor was computed following the equation proposed by Byizigiro et al. (2020). Finally, the K factor was computed using Equation (2) as presented below.

Where R is the rainfall erosivity factor (MJ mmha-1h-1) and P is the mean annual rainfall (mm).

Soil Erodibility Factor

The soil erodibility factor (K) indicates the soil's susceptibility to detachment and transport by runoff, mainly governed by its texture, organic carbon content, and permeability (Pham et al., 2018). Using soil laboratory results for organic carbon and texture, the K factor was computed following the equation proposed by Byizigiro et al. (2020). Finally, the K factor was computed using Equation (2) as presented below.

$$K_{Factor} = f_{sand.} f_{clay.} f_{orgc.} f_{silt.} * 0.1317$$

$$f_{sand.} = 0.2 + 0.3. \, exp\,[-0.256. \, m_{sand.} \, (1 - \frac{m_{silt}}{100})]]$$

$$f_{clay} = \left(\frac{m_{silt}}{m_{clay} + m_{silt}}\right)^{0.3}$$

$$f_{Orgc} = \left(1 - \frac{0.0256.Orgc}{Orgc + exp[3.72 - 2.95.Orgc]}\right)$$

$$f_{silt} = \left(1 - \frac{0.7\left(1 - \frac{m_{sand}}{100}\right)}{\left(1 - \frac{m_{sand}}{100}\right) + exp\left[-5.51 + 22.9.\left(1 - \frac{m_{sand}}{100}\right)\right]}\right)$$

Where *mSand*, *mSilt*, and *mClay* represent the percentages of sand, silt, and clay respectively, and *orgC* is the percentage of organic carbon in the soil layer.

Topographic Factor

The LS factor represents the influence of slope length and steepness on erosion rates, as steeper and longer slopes accelerate water flow, increasing the detachment and transport of soil particles; it is crucial for accurately modeling erosion risk in topographically diverse watersheds (Pham *et al*., 2018 and Koirala *et al*., 2019). Finally, the LS factor was computed using Equation (3) as presented below.

$$LS = Pow\left(\text{"flowacc"} * \frac{[\text{cell resolution}]}{22.13 * 0.4}\right) * \frac{Power\left(Sin\left(\text{"sloperasterdeg"} * 0.01745\right)\right)}{(0.0896, 1.4) * 1.4} \quad (3)$$

Management Factor

The Cover and Management (C) factor represents the ratio of soil loss under specific vegetation or land management to that from bare land, reflecting the protective role of crop cover in reducing erosion (Pham *et al*., 2018). Finally, after the LULC of the selected watershed were conducted the C factor values were assigned according to standard assigned by different authors (Table 3).

Table 3. Land use/cover, area coverage and published C-values.

LUC Type	C-Value
Forest land	0.001
Shrub land	0.014
Cultivated land	0.25
Grass land	0.05
Built-up area	0.05
Bare land	0.45
Settlement	1.0

Support and Conservation Practice (P) Factor

The Support and Conservation Practice (P) factor quantifies the impact of land management practices on reducing soil erosion, ranging from 0 (effective control) to 1 (no control), and was estimated using slope and LULC data due to limited conservation measures in the watershed (Belayneh., 2019). Finally, the P factor values were assigned according to standard assigned by different authors (Table 4).

Table 4. Land management factor (P) values.

Land-Use Type	Slope	P Factor
Agricultural land	0–5	0.1
	5–10	0.12
	10–20	0.14
	20–30	0.19
	30–50	0.25
	50–100	0.33
Other Land	All	1.00

Soil Loss Analysis

The RUSLE model, integrated with ArcGIS Raster Calculator, effectively estimates soil erosion by combining factors like rainfall, soil type, topography, and land cover, providing a spatially explicit analysis. Finally, the soil loss map, calculated using the equation in ArcGIS Raster Calculator, provides an accurate representation of soil erosion severity, pinpointing high-risk areas for targeted conservation interventions (equation 4 and figure 3).

$$A = LS * R * K * C * P \quad (4)$$

where A is annual soil loss (t/ha/year), determined by rainfall erosivity (R), soil erodibility (K), slope length (LS), cover-management (C), and conservation practice (P) factors.

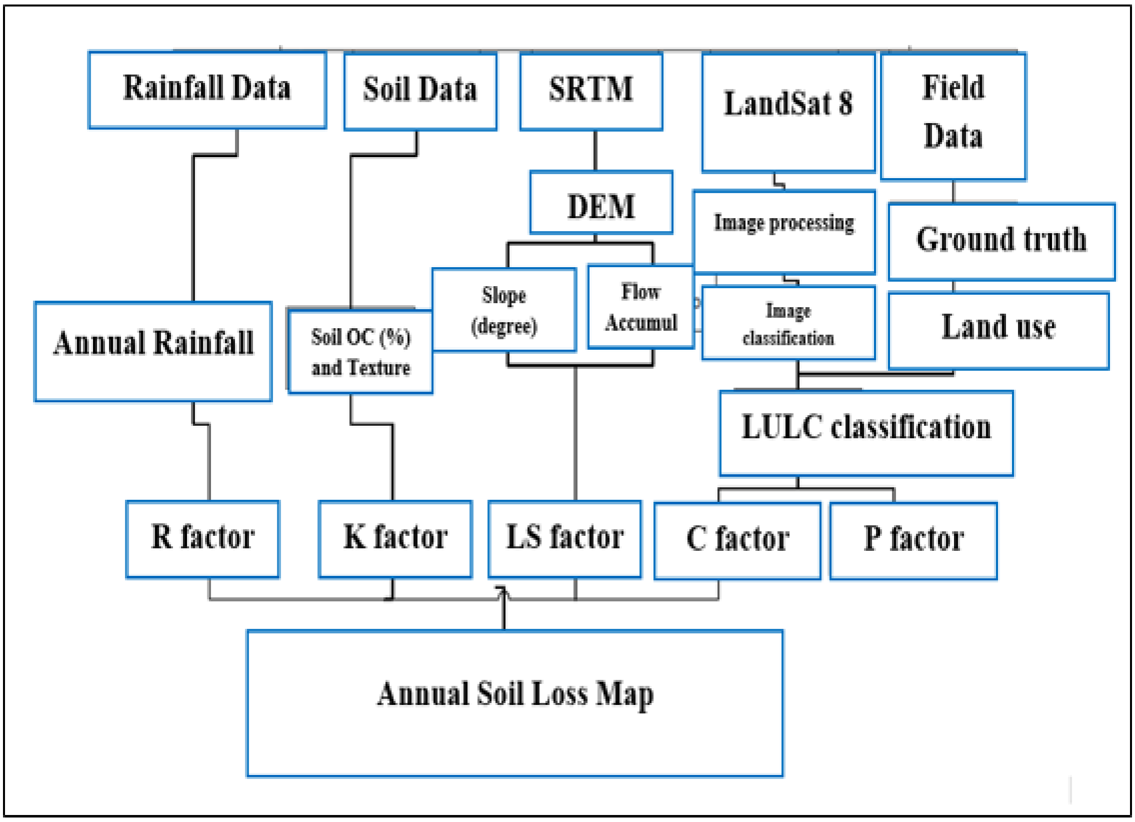

Fig. 3. The overall flow chart of data collection and analysis.

III. Result and Discussion

Factors for Soil Loss Calculation

Rainfall Erosivity (R Factor)

Rainfall erosivity (R factor) plays a crucial role in soil erosion, particularly in areas experiencing high-intensity rainfall. In the study area, the R-factor values range from 661.754 to 1247.83 (Figure 4), indicating a significant potential for soil degradation. The intensity and frequency of rainfall contribute directly to soil detachment and surface runoff, making rainfall one of the dominant drivers of erosion compared to other factors. Higher R-factor values correspond to greater susceptibility to erosion, whereas lower values indicate a reduced risk. Recent studies conducted by Maqsoom *et al* (2020); Wu *et al* (2020); Kerbe *et al* (2023); Abdeta *et al* (2025) have also demonstrated a strong correlation between rainfall amount and erosivity, reinforcing the link between high precipitation intensity and increased soil erosion risk.

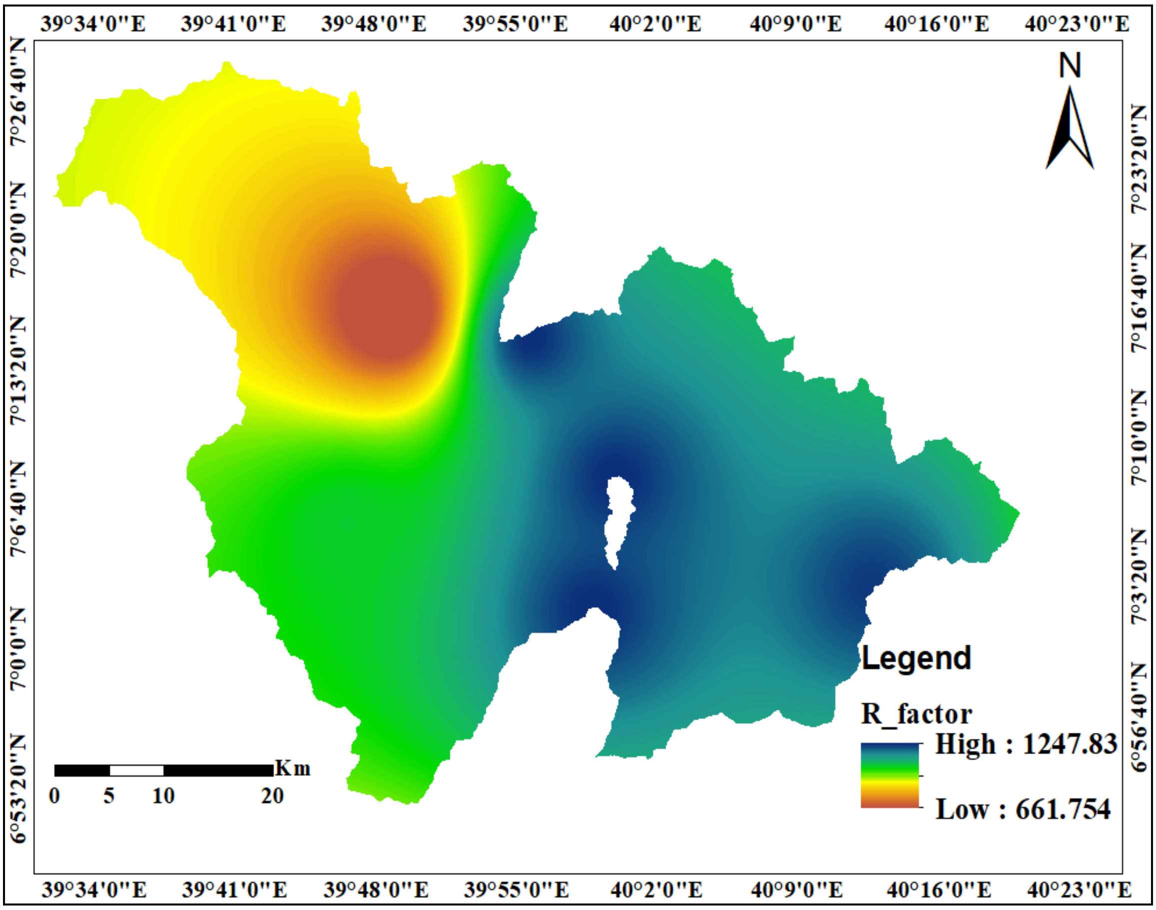

Fig. 4. R factor Map of the watershed.

Slope Length and Steepness (LS Factor)

The LS factor quantifies how length and gradient drive soil erosion slope. In this study, values ranged from 0 to 31.08 (Figure 5), highlighting significant topographic influence. Steeper and longer slopes amplify runoff velocity and sediment transport, intensifying erosion. Greater slope steepness increases flow energy, while extended slopes prolong water accumulation, compounding soil loss. Areas with high LS factor values experience pronounced erosion due to the greater gravitational force exerted on soil particles, reducing infiltration and promoting surface runoff. Steep and extended slopes also exacerbate the transport capacity of runoff, leading to excessive soil displacement and sediment loss, which significantly depletes soil fertility and threatens sustainable land productivity. This finding is consistent with prior research (Yuan *et al*., 2024; Shi *et al*., 2024; Wang *et al*., 2024; Abdeta *et al*., 2025), which collectively affirm that soil erosion severity escalates in direct proportion to increases in slope steepness and length, reinforcing the necessity for targeted soil conservation measures in vulnerable watershed.

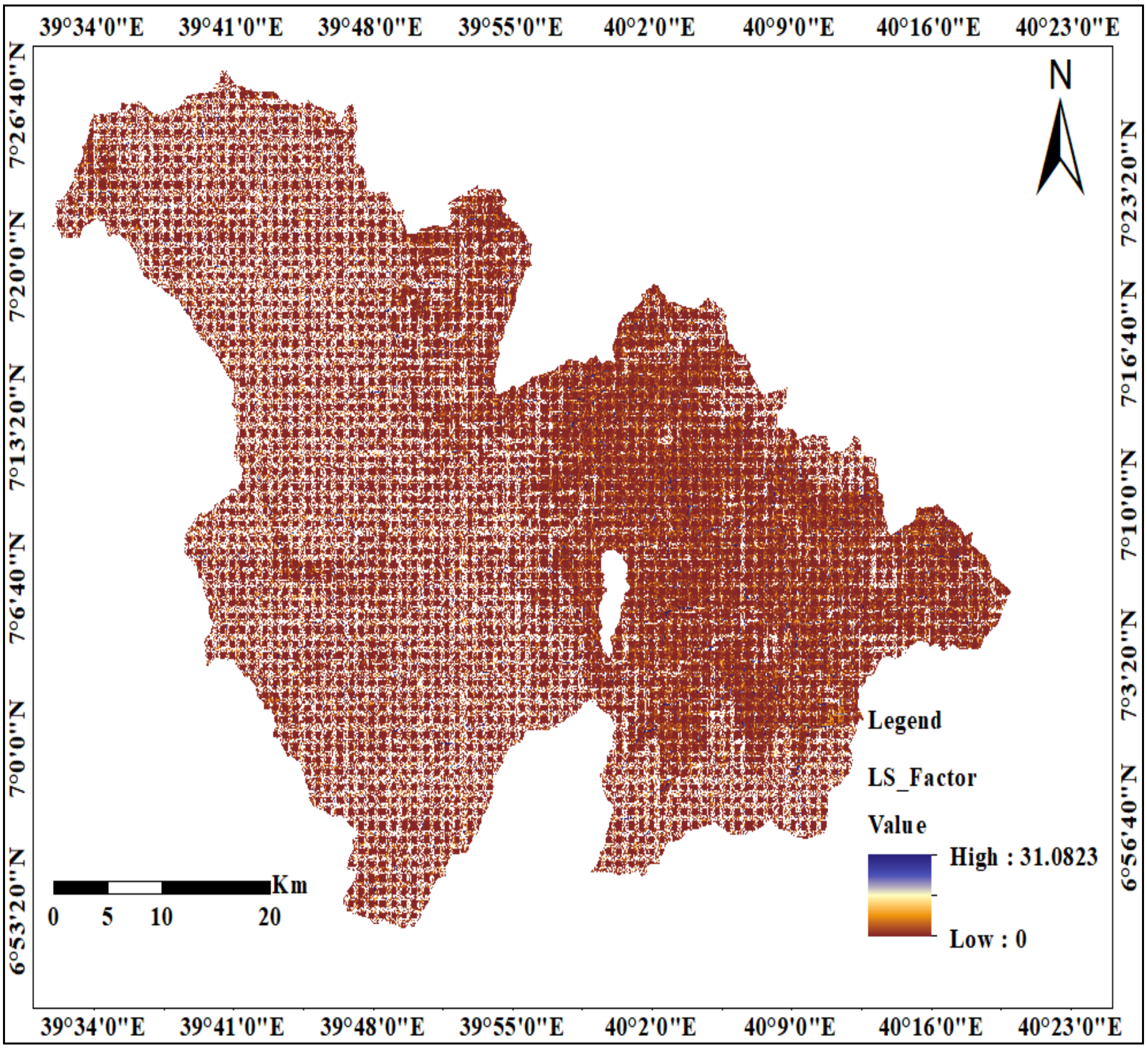

Fig. 5. LS factor map of the watershed.

Soil Erodibility (K Factor)

In this study, the soil erodibility factor (K) exhibited considerable variation, ranging from 0.857 to 2.889 (Figure 6). A higher K value, such as 2.889, signifies a greater vulnerability to soil erosion, whereas a lower value of 0.857 indicates a relatively more resilient soil structure with reduced susceptibility to erosion. The increased erodibility values are directly linked to poor soil aggregation, minimal organic matter content, and reduced structural stability, all of which contribute to excessive soil detachment and transport.

Soils with elevated K-factor values tend to be more fragile due to the lack of cohesive binding agents, particularly humus and organic residues, which play a crucial role in enhancing soil structure and resistance to erosive forces. The deficiency of organic matter exacerbates the breakdown of soil aggregates, increasing susceptibility to both water and wind erosion. Consequently, the presence of highly erodible soils amplifies the risk of land degradation, loss of productive topsoil, and subsequent declines in agricultural productivity. These findings align with previous research Maqsoom *et al* (2020); Hishamunda *et al* (2024); Abdeta *et al* (2025), which collectively underscore the direct correlation between soil erodibility, organic matter depletion, and heightened soil loss.

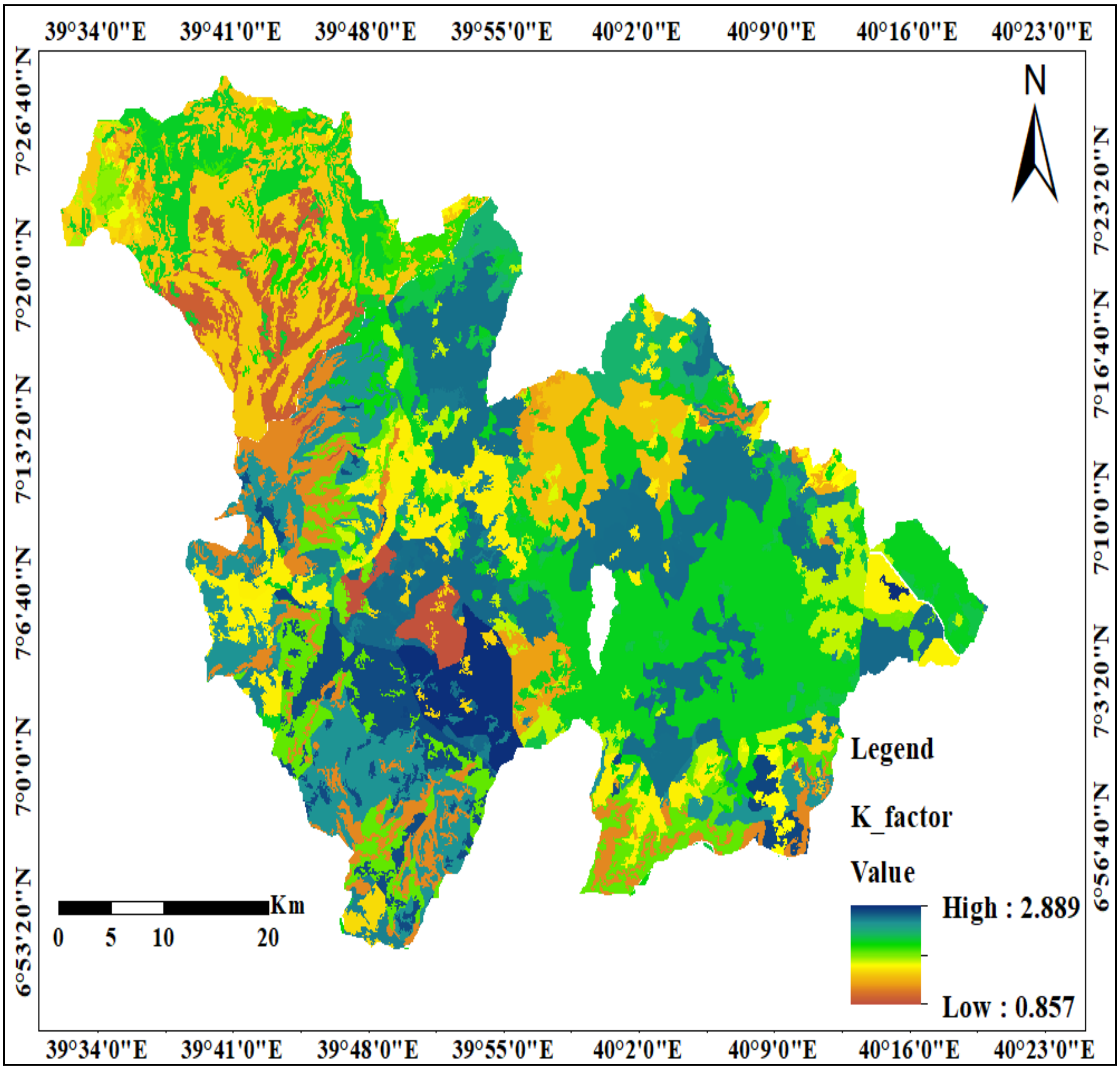

Fig. 6. K factor map of the watershed.

Cover and Management (C Factor)

The C-factor values in the study area range from 0.001 to 1 (Figure 7), highlighting substantial differences in land cover and land management practices. Farmlands exhibit the highest C-factor value (1), indicating maximum vulnerability to soil erosion due to continuous soil disturbances, minimal vegetation cover, and reduced organic matter content. These conditions accelerate soil detachment and runoff, making farmland the most erosion-prone land use category. In contrast, other land use types, such as forests and grasslands, exhibit lower C-factor values, signifying enhanced soil protection, better organic matter retention, and reduced erosion risk. The presence of dense vegetation and root systems in these areas plays a critical role in stabilizing soil and reducing surface runoff.

These findings strongly align with previous studies by Masha and Bojago (2023) and Abdeta *et al* (2025), which also confirmed that farmland is significantly more susceptible to soil erosion compared to other land use classes. This underscores the necessity for integrated soil conservation measures, such as agroforestry, cover cropping, and conservation tillage, to mitigate soil loss in agricultural landscapes and enhance long-term soil productivity.

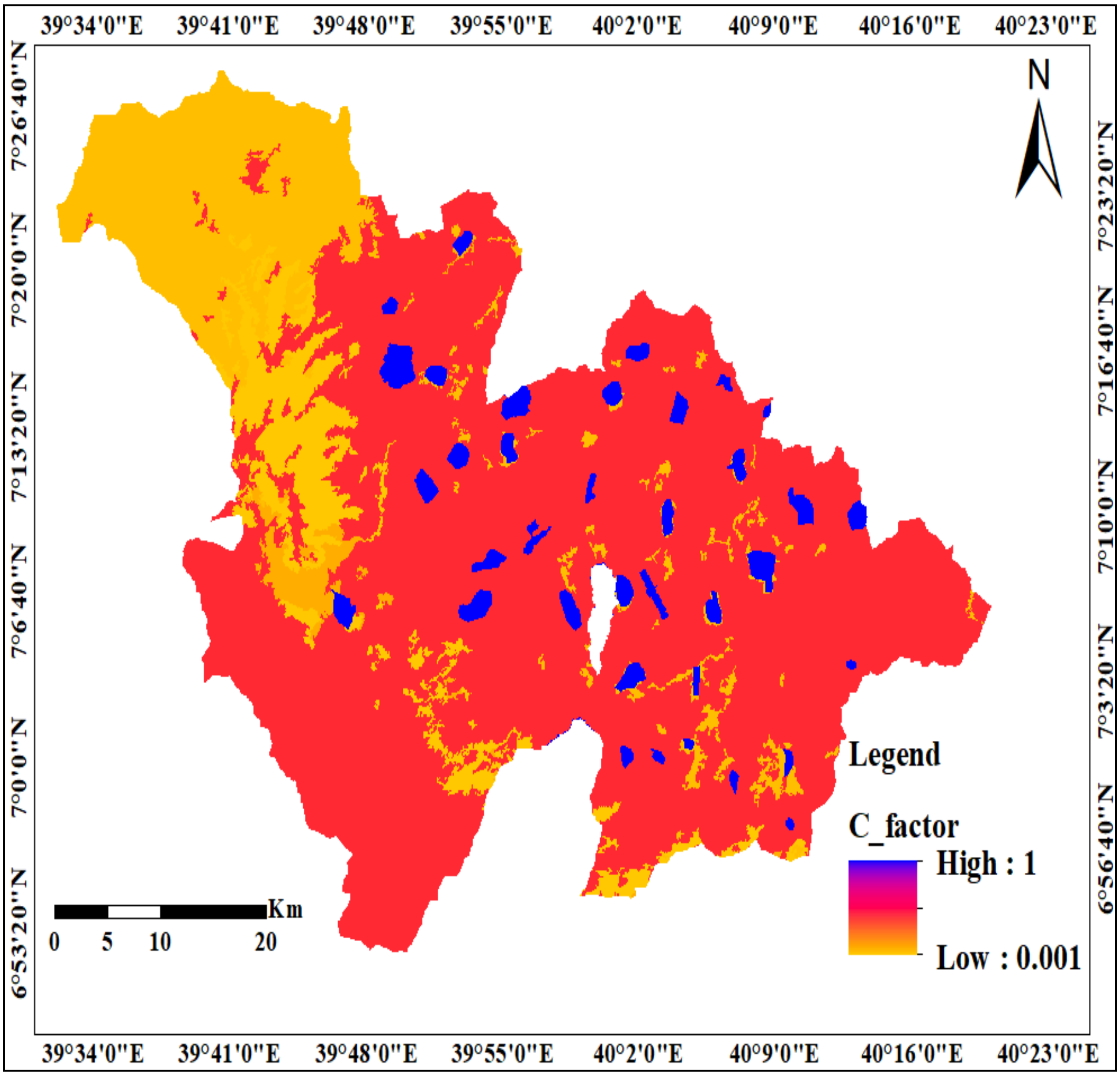

Fig. 7. C factor map of the watershed.

Conservation Practice (P-Factor)

The P-factor values within the watershed range from 0.1 to 1 (Figure 8), reflecting the effectiveness of soil conservation measures across different land uses. The highest P-factor value (1) is observed in farmland, indicating minimal or no erosion control practices, making it highly susceptible to soil loss. In contrast, forest land exhibits the lowest P-factor (0.1), demonstrating its superior natural erosion control through dense vegetation cover and organic matter retention. This finding is consistent with the studies of Tian *et al* (2021), Kerbe *et al* (2023), and Abdeta *et al* (2025), which reported that forest cover lands have the lowest P-factor compared to other land uses such as grasslands, bare lands, and settlement areas. This reinforces the role of the P-factor in representing the effectiveness of soil erosion control measures across different landscapes.

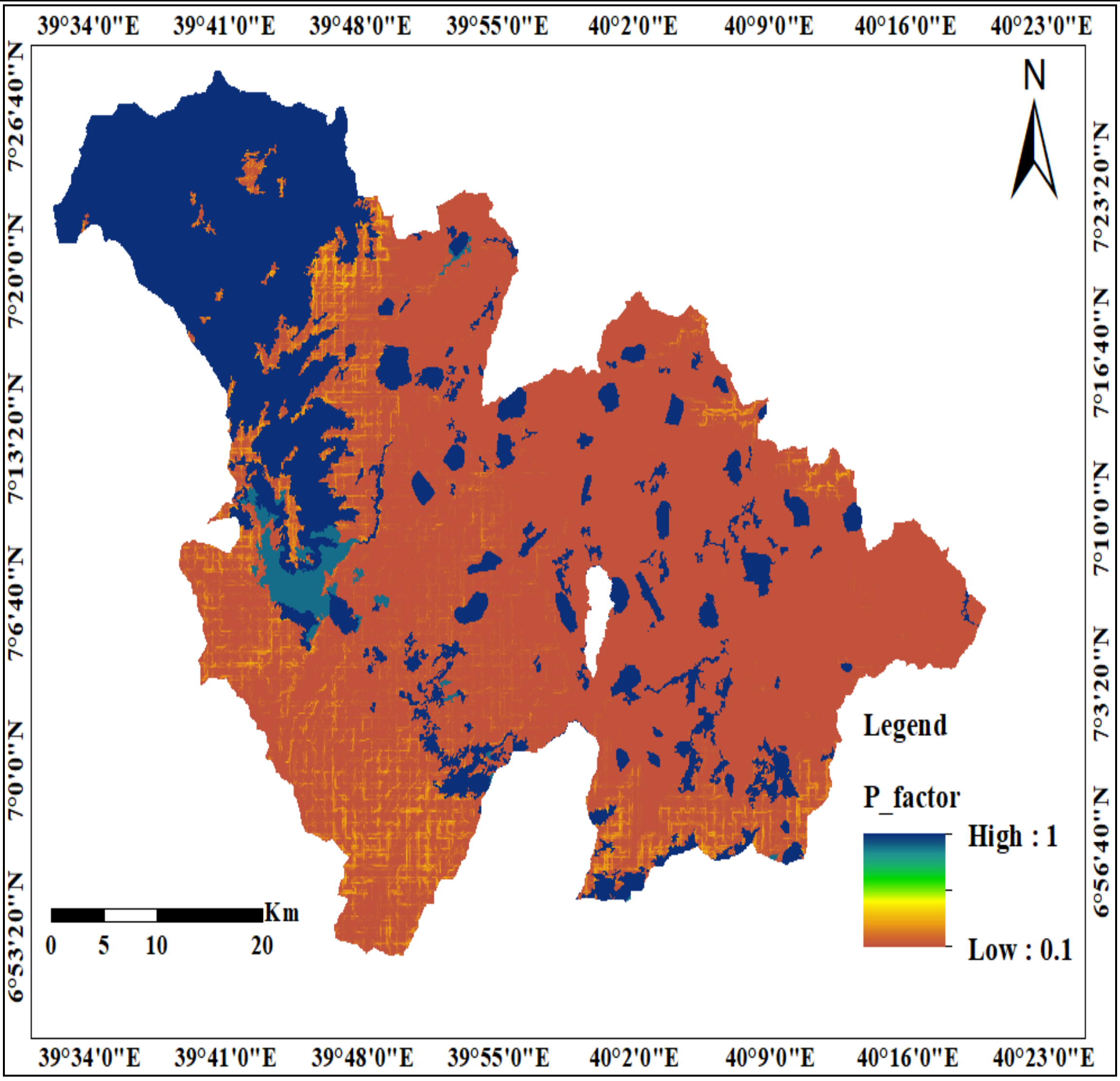

Fig. 8. P factor map of the watershed.

Soil Loss Classification and Conservation Prioritization

The majority of the area (82.84%) experiences slight soil loss (0–11 t/ha/year), indicating stable land with minimal erosion risk, requiring only preventive conservation (Table 5 and Figure 9). Moderate (5.58%) and high soil loss (4.56%) zones show increasing degradation, needing targeted and urgent interventions to maintain productivity (Table 5 and Figure 9). Very high (2.55%) and severe (4.47%) loss areas are critically degraded and demand intensive soil restoration and structural conservation efforts. Prioritizing actions based on erosion severity ensures efficient use of resources and sustainable land management. Watershed erosion severity followed this order: WS1 < WS2 < WS4 < WS3 < WS8 < WS6 < WS7 < WS5 < WS10 < WS9, with WS9 and WS10 facing the highest erosion risks (Figure 9).

The watershed erosion ranking clearly identifies WS9 and WS10 as the most erosion-prone areas. Their high severity levels indicate intense soil degradation, threatening land productivity and ecosystem stability. Prioritizing these watersheds for immediate conservation efforts is essential to reduce further soil loss, restore degraded land, and sustain agricultural potential. The spatial pattern shows most land faces slight erosion, but nearly 17% suffers moderate to severe loss. This highlights the need for urgent, site-specific SWC interventions.

Severely affected areas demand immediate action, while slight/moderate zones need preventive care. A priority-based approach ensures efficient resource use and sustained land productivity.

Table 5. Annual soil loss rates and severity classes.

Soil Loss Rate (ton $ha^{-1}year^{-1}$)	Soil Loss Severity Classes	Area	
		(ha)	(%)
0 –11	Slight	167069.80	82.84
11 – 18	Moderate	11253.40	5.58
18 – 30	High	9193.71	4.56
30 – 50	Very high	5145.37	2.55
>50	Severe	9019.12	4.47

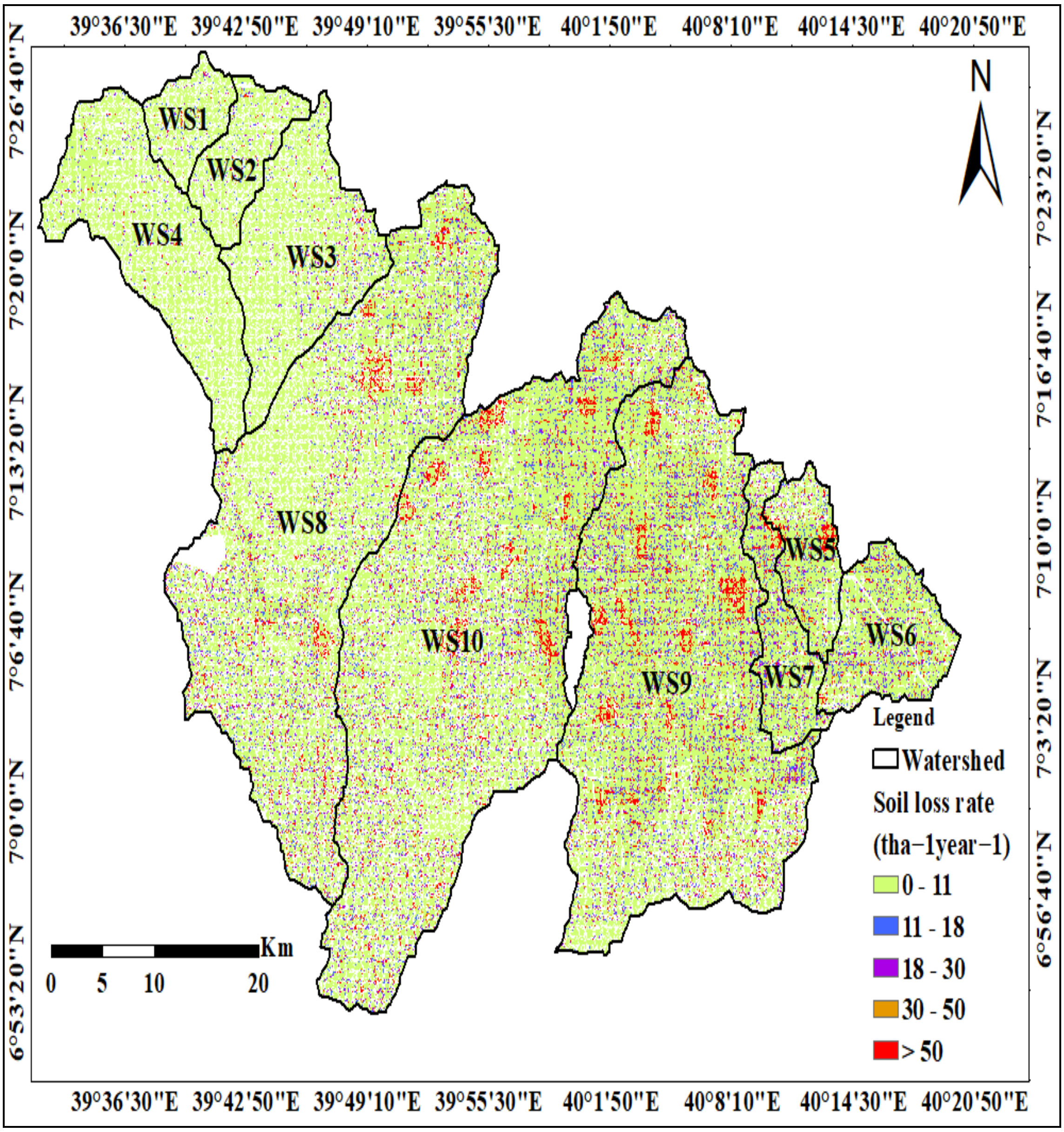

Fig. 9. Annual Soil loss rates for the selected sub-watersheds of Bale Highland.

Soil Loss from the Sub-Watersheds

Table 3 provides essential data on soil loss distribution across ten sub-watersheds, enabling the identification of erosion hotspots and guiding the prioritization of targeted soil and water conservation measures based on area size, erosion severity, and variability. The results show that WS9 and WS10 are the largest sub-watersheds, covering over 53% of the total area and contributing nearly 56.5% of total soil loss (Table 6 and Figure 10). Their high mean soil loss rates (1.412-1.477 t/ha/year) and large standard deviations (1.05-1.13) indicate severe and variable erosion, making them priority areas for soil and water conservation interventions.

WS5, though only 2.53% of the watershed, contributes 2.73% of total soil loss with a high mean erosion rate (1.476 t/ha/year), indicating severe localized degradation that requires targeted interventions (Table 6 and Figure 10). WS8, covering 21.27% of the area and contributing 20.92% of soil loss, shows consistent erosion across a broad area (mean: 1.341 t/ha/year), making it a secondary priority for conservation due to its large sediment yield and potential downstream impacts (Table 6 and Figure 10).

WS1 to WS4 cover small areas with low soil loss rates (1.061-1.121 t/ha/year) and contribute only 12.26% of total sediment. Continued protection is essential to sustain their current stability. WS6 and WS7 show moderate erosion (1.350-1.418 t/ha/year) with notable variability and contribute 7.63% of sediment from 7.54% of the area. Their erosion risk warrants proactive conservation measures (Table 6 and Figure 10). The standard deviation values highlight the variability in soil loss across sub-watersheds. Higher values, like in WS5 (1.17) and WS9 (1.13), indicate areas with greater soil loss variation, suggesting localized erosion hotspots. In contrast, lower values, such as in WS4 (0.37), reflect more uniform erosion, potentially due to consistent land cover or topography. This variability underscores the need for specific soil conservation approaches for each sub-watershed.

Table 6. Soil loss for the sub-watersheds.

Sub-Watershed	Area (ha)	Area (%)	Mean ($tha^{-1}year^{-1}$)	Sum ($tha^{-1}year^{-1}$)	Sum (%)	Standard Deviation
WS1	29704500	1.48	1.086	35843.00	1.18	0.42
WS2	40590000	2.03	1.092	49228.00	1.62	0.46
WS3	112228200	5.60	1.121	139742.00	4.61	0.52
WS4	124794900	6.23	1.061	147120.00	4.85	0.37
WS5	50575500	2.53	1.476	82925.00	2.73	1.17
WS6	85604400	4.27	1.350	128414.00	4.23	0.88
WS7	65510100	3.27	1.418	103220.00	3.40	1.01
WS8	425864700	21.27	1.341	634709.00	20.92	0.94
WS9	524907900	26.21	1.477	861409.00	28.39	1.13
WS10	542829600	27.11	1.412	851679.00	28.07	1.05

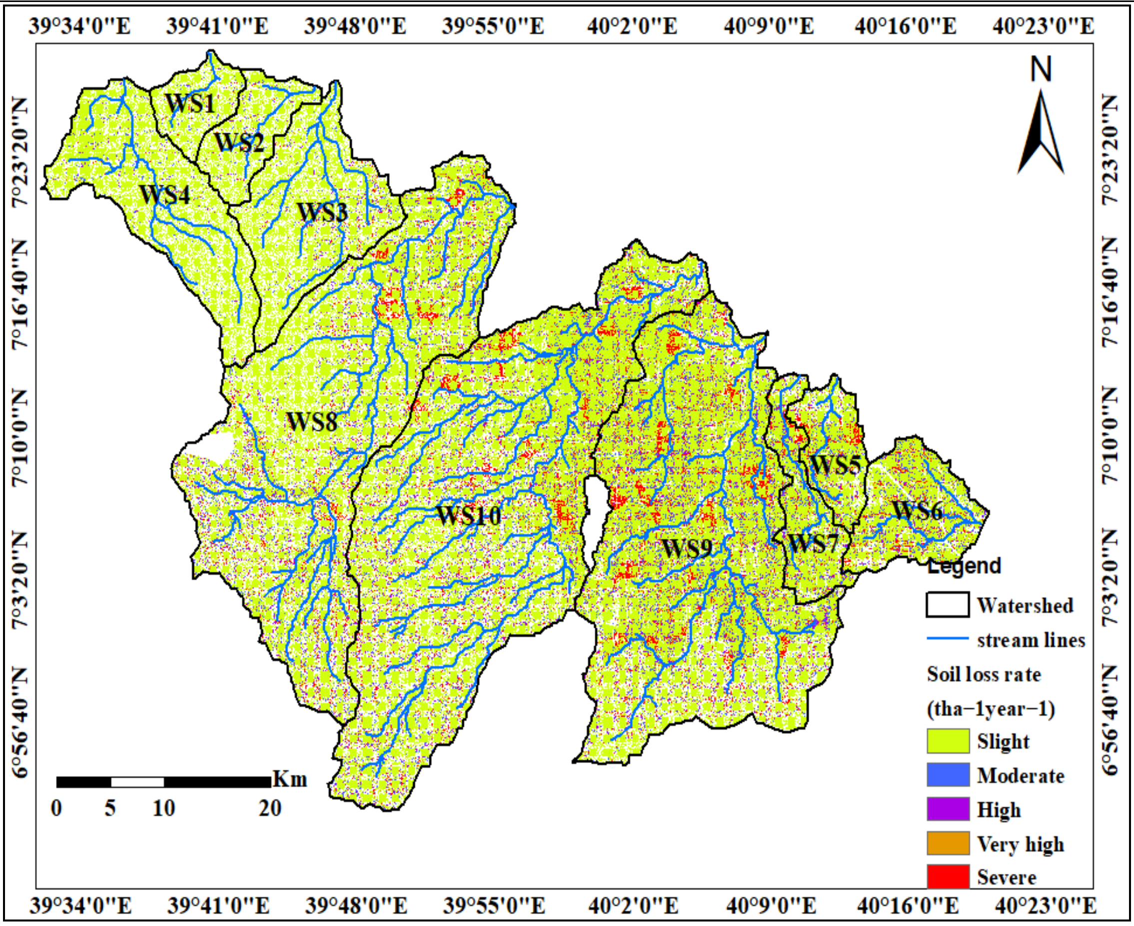

Fig. 10. Soil loss severity classes for the selected sub-watersheds of Bale Highland.

IV. Conclusion and Recommendation

Conclusion

Effective soil and water conservation requires tailored interventions that consider the spatial distribution and intensity of erosion within each sub-watershed. The majority of the area (82.84%) is under slight soil loss, indicating stable conditions with minimal intervention needs. However, moderate to high loss zones (10.14%) signal emerging degradation and require targeted conservation measures. Critically degraded areas (7.02%) demand urgent and intensive restoration to prevent irreversible productivity loss.

Watershed erosion ranking (WS1 < WS2 < WS4 < WS3 < WS8 < WS6 < WS7 < WS5 < WS10 < WS9) clearly identifies WS9 and WS10 as the most erosion-prone areas. The findings provide a solid basis for targeted conservation planning, highlighting the value of RUSLE-integrated geospatial analysis as a decision-support tool for prioritizing soil and water management in high-risk erosion zones.

Intensive soil and water conservation interventions should be prioritized in sub-watersheds WS9 and WS10 due to their high vulnerability to degradation. Sub-watershed WS5 requires close monitoring and adaptive management to prevent further deterioration. Moderate conservation measures should be applied in WS6, WS7, and WS8 to address emerging risks and maintain stability. Meanwhile, the relatively stable sub-watersheds WS1 to WS4 should continue to receive routine protective management to sustain their current condition and prevent future degradation.

V. Recommendations

- WS9 and WS10 should be prioritized for intensive soil and water conservation efforts. These sub-watersheds cover large areas and experience significant soil loss. Interventions should include structural measures such as terracing, check dams, and silt traps, along with biological measures like cover cropping and agroforestry to stabilize the soil.
- WS5 should be monitored closely due to localized erosion hotspots. Targeted interventions like contour farming, erosion control bunds, and vegetative cover can address these vulnerable zones, preventing further degradation.
- WS8, WS6, and WS7 require moderate interventions, particularly focusing on areas where erosion is variable. These sub-watersheds can benefit from integrated soil and water conservation techniques, including contour farming and the planting of drought-resistant species.
- WS1 to WS4 are relatively stable but should not be neglected. Routine monitoring and ongoing protective measures, such as agroforestry and maintaining ground cover, will help sustain their stability and prevent future degradation.
- Generally, soil loss and soil erosion severity mapping developed using RUSLE model and geospatial technique is a key tool for decision-making for effective and proper soil and water conservation innervations.
- Further research should focus on combined uses of RUSLE model and geospatial technique with on spot long-term soil erosion and soil loss data measured recommended.

Acknowledgments

The authors sincerely thank the Oromia Agricultural Research Institute for financial support and the Sinana Agricultural Research Center for vital logistical assistance. They also extend heartfelt appreciation to all who contributed to the successful completion of this study.

References

[1] Abdeta Tolassa Fayisa, Wondafrash Genet Degu, Ajay Babu Gangidi and Dessalegn Obsi Gemeda. 2025. Soil loss estimation using RUSLE model and geospatial technologies in Gulufa Watershed, Dabus Sub-basin, and West Ethiopia. *Sustainable Environment*, 11(1), p.2464402.
[2] Arabameri, A., Asadi Nalivan, O., Chandra Pal, S., Chakrabortty, R., Saha, A., Lee, S., Pradhan, B. and Tien Bui, D., 2020. Novel machine learning approaches for modelling the gully erosion susceptibility. *Remote Sensing*, *12*(17), p.2833.
[3] Belayneh, M., Yirgu, T. and Tsegaye, D., 2019. Potential soil erosion estimation and area prioritization for better conservation planning in Gumara watershed using RUSLE and GIS techniques'. *Environmental Systems Research*, *8*(1), pp.1-17.
[4] Bewket, W. and Sterk, G., 2005. Dynamics in land cover and its effect on stream flow in the Chemoga watershed, Blue Nile basin, Ethiopia. *Hydrological Processes: An International Journal*, *19*(2), pp.445-458.
[5] Byizigiro, R.V., Rwanyiziri, G., Mugabowindekwe, M., Kagoyire, C. and Biryabarema, M., 2020. Estimation of soil erosion using RUSLE model and GIS: The case of Satinskyi catchment, western Rwanda. *Rwanda Journal of Engineering, Science, Technology and Environment*, *3*(1).
[6] FAO. 1986. Ethiopian Hihgland Reclamation Study: Report prepared for the government of Ethiopia. Vol. I.
[7] Hishamunda, S., Fashaho, A., Uwihirwe, J., Bugenimana, E.D., Musinga, C.M. and Munyandamutsa, P., 2024. Controlling soil erosion and landslides through ecosystem-based adaptation interventions in the hilly landscape of western Rwanda. *Soil Advances*, *2*, p.100020.
[8] Hurni H. 1985. Erosion productivity conservation systems in Ethiopia. Paper Presented at the 4th International Conference on Soil Conservation. 3-9 November 1985, Maracacy, Venezuela.
[9] Kerbe, T.A., Mosissa Ejeta, T. and Gemeda, D.O., 2023. Soil erosion risk assessment using geospatial technologies and RUSLE model in Bore Guda Watershed, Southwestern Ethiopia. *Geology, Ecology, and Landscapes*, pp.1-13.
[10] Koirala, P., Thakuri, S., Joshi, S. and Chauhan, R., 2019. Estimation of soil erosion in Nepal using a RUSLE modeling and geospatial tool. *Geosciences*, *9*(4), p.147.

[11] Li, N., Zhao, H., Luo, Z., Wang, T., Yang, J., Li, L. and Que, S., 2024. Soil erosion prediction in multiple scenarios based on climate change and land use regulation policies in context of sustainable agriculture. *Catena*, *247*, p.108525.

[12] Luvai, A., Obiero, J. and Omuto, C., 2022. Soil loss assessment using the revised universal soil loss equation (RUSLE) model. *Applied and Environmental Soil Science*, *2022*(1), p.2122554.

[13] Masha, M. and Bojago, E., 2023. Evaluating soil erosion and determinants of farmers' adoption of soil and water conservation measures in the Offa district, southern Ethiopia. *Journal of Agriculture and Food Research*, *14*, p.100866.

[14] Olika, G., Fikadu, G. and Gedefa, B., 2023. GIS based soil loss assessment using RUSLE model: A case of Horo district, western Ethiopia. *Heliyon*, *9*(2).

[15] Pham, T.G., Degener, J. and Kappas, M., 2018. Integrated universal soil loss equation (USLE) and Geographical Information System (GIS) for soil erosion estimation in A Sap basin: Central Vietnam. *International Soil and Water Conservation Research*, *6*(2), pp.99-110.

[16] Renard KG Foster GR Weesies GA McCool DK and Yoder DC 1997. Predicting soil erosion by water: a guide to conservation planning with the revised universal soil loss equation (RUSLE). US Department of Agriculture Agricultural Handbook No. 703. USDA Washington DC.

[17] Shi, J., Zhang, Z., Wang, Z., Peng, Y. and Wang, X., 2024. Soil erosion alters the composition of soil nitrogen and induces nitrogen immobilization along a sloping agricultural landscape. *Soil Use and Management*, *40*(2), p.e13067.

[18] Sodoke, S., Andam-Akorful, S.A., Amuah, E.E.Y., Amoah, E.G., Anokye, K., Nang, D.B. and Kazapoe, R.W., 2025. GIS-based assessment of soil erosion impact and mitigation strategies for sustainable agriculture in Ghana's most vulnerable region. *Environmental and Sustainability Indicators*, *25*, p.100551.

[19] Stefanidis, S., Alexandridis, V., Spalevic, V. and Mincato, R.L., 2022. Wildfire effects on soil erosion dynamics: the case of 2021 megafires in Greece. *Agriculture and Forestry/Poljoprivreda i šumarstv*, *68*(2).

[20] Stefano Di, C., Nicosia, A., Pampalone, V. and Ferro, V., 2023. Soil loss tolerance in the context of the European Green Deal. *Heliyon*, *9*(1).

[21] Sud, A., Sajan, B., Kanga, S., Singh, S.K., Singh, S., Durin, B., Kumar, P., Meraj, G., Sahariah, D., Debnath, J. and Chand, K., 2024. Integrating RUSLE model with cloud-based geospatial analysis: a google earth engine approach for soil erosion assessment in the Satluj watershed. *Water*, *16*(8), p.1073.

[22] Tesfaye, G., Debebe, Y. and Fikirie, K., 2018. Soil erosion risk assessment using GIS based USLE model for soil and water conservation planning in Somodo watershed, south West Ethiopia. *Int J Environ Agric Res*, *4*(5), pp. 35-43.

[23] Thakuriah, G., 2023. GIS-based revised universal soil loss equation for estimating annual soil erosion: a case of lower Kulsi basin, India. *SN Applied Sciences*, *5*(3), p.81.

[24] Wang, K., Zhou, J., Tan, M.L., Lu, P., Xue, Z., Liu, M. and Wang, X., 2024. Impacts of vegetation restoration on soil erosion in the Yellow River Basin, China. *Catena*, *234*, p.107547.

[25] Wu, G.L., Liu, Y.F., Cui, Z., Liu, Y., Shi, Z.H., Yin, R. and Kardol, P., 2020. Trade-off between vegetation type, soil erosion control and surface water in global semi-arid regions: A meta-analysis. *Journal of Applied Ecology*, *57*(5), pp.875-885.

[26] Yuan, S., Xu, Q., Zhao, K., Zhou, Q., Wang, X., Zhang, X., Chen, W. and Ji, X., 2024. Dynamic analyses of soil erosion and improved potential combining topography and socio-economic factors on the Loess Plateau. *Ecological Indicators*, *160*, p.111814.

AUTHOR'S PROFILE

First Author
Mulugeta Eshetu, Sinana Agricultural Research Center, Soil Fertility Improvement, Soil and Water Conservation and Watershed Management Team, P. O. Box 208, Bale-Robe, Ethiopia.

Second Author
Tesfaye Ketema, Sinana Agricultural Research Center, Soil Fertility Improvement, Soil and Water Conservation and Watershed Management Team, P. O. Box 208, Bale-Robe, Ethiopia.

Third Author
Regassa Gosa, Sinana Agricultural Research Center, Soil Fertility Improvement, Soil and Water Conservation and Watershed Management Team, P. O. Box 208, Bale-Robe, Ethiopia.

Fourth Author
Girma Getachew, Sinana Agricultural Research Center, Soil Fertility Improvement, Soil and Water Conservation and Watershed Management Team, P. O. Box 208, Bale-Robe, Ethiopia.